

Ultraviolet and visible range plasmonics of a topological insulator

Jun-Yu Ou,¹ Jin-Kyu So,^{1,*} Giorgio Adamo,² Azat Sulaev,³ Lan Wang,³ and Nikolay I. Zheludev^{1,2}

¹*Optoelectronics Research Centre & Centre for Photonic Metamaterials, University of Southampton, UK*

²*Centre for Disruptive Photonic Technologies, Nanyang Technological University, Singapore 637371, Singapore*

³*School of Physical and Mathematical Sciences, Nanyang Technological University, 637371, Singapore*

The development of metamaterials, data processing circuits and sensors for the visible and UV parts of the spectrum is hampered by the lack of low-loss media supporting plasmonic excitations and drives the intense search for plasmonic materials beyond noble metals. By studying plasmonic nanostructures fabricated on the surface of topological insulator $\text{Bi}_{1.5}\text{Sb}_{0.5}\text{Te}_{1.8}\text{Se}_{1.2}$ we found that it is orders of magnitude better plasmonic material than gold and silver in the blue-UV range. Metamaterial fabricated from $\text{Bi}_{1.5}\text{Sb}_{0.5}\text{Te}_{1.8}\text{Se}_{1.2}$ show plasmonic resonances from 350 nm to 550 nm while surface gratings exhibit cathodoluminescent peaks from 230 nm to 1050 nm. The negative permittivity underpinning plasmonic response is attributed to the combination of bulk interband transitions and surface contribution of the topologically protected states. The importance of our result is in the identification of new mechanisms of negative permittivity in semiconductors where visible-range plasmonics can be directly integrated with electronics.

Plasmons, coupled excitations of electrons in solids and electromagnetic fields, are responsible for brilliant colors of Roman vases and medieval church vitrages delivered by the colloidal suspension of gold particles in glass¹. They are the key to nanophotonic applications and form responses of nanostructured metal surfaces and artificial metamaterial photonic structures. Plasmons can localize electromagnetic energy in the nanoscale which is crucial for the next generation of ultra-high density optically assisted magnetic data storage technology^{2,3}. Plasmons are exploited for enhancement of light-harvesting applications, in particular photovoltaics⁴. Plasmon resonances are used in biological sensors such as the pregnancy test⁵. Plasmon-polaritons propagating on the surface are seen as a promising information carrier for ultra-compact inter-chip interconnects applications⁶⁻⁸ and all-optical data processing chips⁹. However, only a narrow class of materials can support plasmons, most notably noble metals like silver and gold. In recent years, we saw a surge of research aiming to identify new plasmonic media and a very substantial progress has been possible in the search and characterization of infrared plasmonic materials, most notably conductive oxides, nitrides and graphene¹⁰⁻¹². The UV-visible part of the spectrum remains an extremely challenging domain for plasmonics as gold and silver have losses there, while this spectral range remains unattainable for artificially doped semiconductors and graphene¹¹. If a low loss plasmonic media existed for the blue-UV part of the spectrum, this would open a plethora of important applications that could include a long-awaited metamaterial suitable for super-lens with resolution breaking the diffraction limit to operate at optical frequency^{13,14}, a sensor sensitive to specific near-UV resonances in proteins and DNAs, or enhanced light concentrator for even further improvement of the density of optical and optically-assisted data storage¹⁵, just to mention a few. In this work, using the example of $\text{Bi}_{1.5}\text{Sb}_{0.5}\text{Te}_{1.8}\text{Se}_{1.2}$ (BiSbTeSe) topological insulator crystal^{16,17}, we identify a new mechanism of visible and UV plasmonic response which is a combination of surface

optical conductivity residing in a nanoscale layer of topologically protected surface states of the crystal and the new mechanism of bulk optical conductivity related to the dispersion created by the interband transitions in the medium. In a series of optical and cathode-luminescence experiments with unstructured and nanostructured surfaces of the alloy, we show that its plasmonic properties are very well pronounced and are superior to that of metallic gold in the spectral range from 200 nm to ~ 500 nm and to that of silver from 200 nm to ~ 340 nm. In particular, on nanostructured metamaterial surfaces of BiSbTeSe we demonstrated profound plasmonic peaks of absorption from 350 nm to 550 nm, and on grating arrays with periods from 150 nm to 800 nm we observed peaks of plasmonic cathodoluminescence in the wavelength range from 230 nm to 1050 nm.

Plasmonics is often defined as electromagnetism at the interface between dielectrics and conductive media with negative value of the real part of dielectric permittivity ε where external field E induces displacement field D of essentially opposite direction ($D = \varepsilon E$, $\text{Re}\{\varepsilon\} < 0$ and $-\text{Re}\{\varepsilon\} > \text{Im}\{\varepsilon\}$). Under such condition the interfaces can support highly localized oscillation and confined surface waves known as localized plasmons and surface plasmon-polariton waves¹⁸. Plasmons derive their name from plasma of free electrons in metals or heavily doped semiconductors¹⁹⁻²¹ at interfaces of which they are often observed. Despite the huge success of modern plasmonics, the limitation of noble metals as a plasmonic material has led to the search for alternative plasmonic materials^{10,11}. In general, there are two approaches of obtaining plasmonic behavior at the desired frequencies. One is to heavily dope semiconductors to increase their charge carrier concentration, but this approach has been successful only up to near-IR regime due to the difficulty in achieving the required doping level and additional losses at such a high doping level²¹⁻²⁶. The other is to mix metals with non-metals or other metals. Titanium nitride (TiN) which has been revisited recently as a promising plasmonic material for the visible and near-IR

wavelengths falls into this category^{10,27–31}. Apart from the bulk plasmonic materials, two-dimensional plasmonic materials such as 2D electron gas (2DEG) systems^{32–34} or, recently, graphene in the mid-IR regime^{35,36} have been attracting a huge interest due to their unusual properties such as the extreme field confinement³⁷. Topological insulator is a material that behaves as insulator in its interior but whose surface contains conducting states, meaning that electrons can only move along the surface of the material. Thus it also falls into this category of 2D plasmonic materials³⁸ and the plasmons on this 2DEG system has been observed at terahertz frequencies recently³⁹.

Here, we report on the plasmonic behavior of a topological insulator, $\text{Bi}_{1.5}\text{Sb}_{0.5}\text{Te}_{1.8}\text{Se}_{1.2}$, in visible and UV parts of the spectrum. In contrast to the prototypical topological insulators such as Bi_2Se_3 and Bi_2Te_3 , it has a large bulk resistivity due to its ordered Te-Bi-Se-Bi-Te quintuple layers¹⁶. Our $\text{Bi}_{1.5}\text{Sb}_{0.5}\text{Te}_{1.8}\text{Se}_{1.2}$ single crystals were synthesized by melting high-purity (99.9999%) Bi, Sb, Te and Se with molar ratio 1.5:0.5:1.8:1.2 at 950°C in an evacuated quartz tube. The temperature was then gradually decreased to room temperature over a span of three weeks¹⁷. The BSTS single crystal was then cleaved along the (100) family of planes to a thickness of ~ 0.5 nm.

We first investigated the optical properties of the unstructured surface by multiple-angle spectroscopic ellipsometry in the range from 200 nm to 1600 nm, see Fig. 1. To retrieve dielectric function from these measurements, we followed the model that was successfully developed to represent lower frequency conductivity of this topological insulator¹⁷: we assumed a material structure consisting of a bulk semiconductor with a thin metal film on top as shown in the inset of Fig. 1a. The semiconductor bulk substrate supporting the thin film was modeled using the Tauc-Lorentz⁴⁰ model that has been successfully applied to this class of materials in the past⁴¹, while conductivity of the topological insulator film was assumed to obey the Drude dispersion⁴². From our analysis of the spectroscopic data, we found that the best-fit parameters such as band gap of the bulk component, 0.25 eV, thickness of the topological insulator layer, $d = 1.5$ nm and plasma and collision frequencies of Drude model, 7.5 eV and 0.05 eV, respectively, are close to previously reported values found for this material from the independent DC conductivity measurements^{16,17} and corroborate very well with the results of *ab initio* calculations of dielectric functions of similar alloys^{43,44}. We therefore conclude that the proposed layer-on-substrate material structure adequately describes optical properties of $\text{Bi}_{1.5}\text{Sb}_{0.5}\text{Te}_{1.8}\text{Se}_{1.2}$ and use it for the interpretation of plasmonic response of the material.

Negative permittivity of $\text{Bi}_{1.5}\text{Sb}_{0.5}\text{Te}_{1.8}\text{Se}_{1.2}$ is clearly seen between the wavelengths, 200 – 670 nm (Fig. 1a). It is instructive to observe that the negative epsilon regimes in this spectral range are characteristic to both components of the structure, the Drude layer and underlying

bulk semiconductor, as shown in Fig. 1b. However the bulk contribution alone is not sufficient to explain dielectric properties of the material as illustrated in Fig. 1b. The topologically protected surface charge carriers are forming the response of the top metallic layer: if such conductivity would exist in the bulk medium, plasmonic properties of such hypothetical material would be better than that of any known plasmonic material in this spectral range. Here we see that even a thin layer of the topological phase has a profound impact on plasmonic response of the structure even when placed on a lossy substrate. Our analysis of the ellipsometry data shows that it adds up to 8% to the reflectivity of the nanostructured surface.

The bulk plasmonic response here largely originates from the interband absorption dispersion in this material, not from the bulk free carriers. Its origin is similar to that of the negative dielectric permittivity area at the higher frequency wing of the isolated absorption peak that corresponds to the peak in joint density of states in case of semiconductor. It can be understood as an inevitable consequence of the Kramers-Kronig relations that link the real and imaginary parts of permittivity near a strong absorption peak, as has been observed near infrared phonon lines^{45,46}. Negative permittivity due to interband transitions has been theoretically predicted for a similar material of Bi_2Se_3 in electronic structure calculations within the density function theory based on full potential linearized augmented plane wave and local orbitals^{43,44}. However, to our knowledge $\text{Bi}_{1.5}\text{Sb}_{0.5}\text{Te}_{1.8}\text{Se}_{1.2}$ represents the first example of material where negative permittivity due to interband electronic absorption is seen at the optical frequencies experimentally. We argue that negative permittivity due to the strong interband absorption can only be seen in semiconductors where background, zero-frequency permittivity is small enough to be overcome by negative resonant contribution and $\text{Bi}_{1.5}\text{Sb}_{0.5}\text{Te}_{1.8}\text{Se}_{1.2}$ is the first known example.

To evaluate the competitiveness of $\text{Bi}_{1.5}\text{Sb}_{0.5}\text{Te}_{1.8}\text{Se}_{1.2}$ as a plasmonic material at the optical frequencies we computed the quality factors for surface plasmon polaritons, Q^{10} . Fig. 1c shows the plasmonic quality factors for the $\text{Bi}_{1.5}\text{Sb}_{0.5}\text{Te}_{1.8}\text{Se}_{1.2}$ crystal (Fig. 1a) and widely accepted data for noble metals^{47,48}. From there we argue that the topological insulator is a better plasmonic material than silver and gold in 200 – 350 nm and 200 – 500 nm, respectively. Good quality factors for plasmonic resonances could be expected in nanostructures fabricated from $\text{Bi}_{1.5}\text{Sb}_{0.5}\text{Te}_{1.8}\text{Se}_{1.2}$ in the range from 250 to 600 nm and this is what we have illustrated further.

To verify the plasmonic behavior of $\text{Bi}_{1.5}\text{Sb}_{0.5}\text{Te}_{1.8}\text{Se}_{1.2}$ in nanostructures we manufactured a series metamaterials, nano-slit antenna arrays with linear grooves cut into the surface of the crystal and gratings on the crystal surface using focused-ion-beam milling (Fig. 2). In the nano-slit antenna array the slit length D was varied from 100 nm to 400 nm and the

period of the slit (unit cell size, UC) was kept at 300 nm for $D = 100 - 225$ nm and $UC = 1.5D$ for $D = 250 - 400$ nm. The fabricated nano-slits' profile is close to V-shape, as shown in Fig. 2b.

The plasmonic response of the fabricated nano-slit metamaterials and gratings were studied by measuring their reflection spectra $R(\lambda)$ and their corresponding absorption spectra $A(\lambda) = 1 - R(\lambda)$ for two incident polarizations perpendicular and parallel to the nano-slits (Figures 3a and 3b). The nano-slit arrays clearly exhibited plasmonic colors for light polarized perpendicularly to the slits, as can be seen in the optical microscope images (see Fig. 2d). A profound resonance in plasmonic absorption can be seen for this polarization (Fig. 3a). Indeed, if a wire dipole is resonant for light polarized along the dipole, according to the Babinet principle, slits in the conductive surface, the "anti-dipole", will be resonant for perpendicular polarization. Here, the resonant wavelength increases monotonously with the length of the groove as can be seen in Fig. 3c. As expected, no plasmonic resonance can be found in the polarization along the groove (see Fig. 3b). On all graphs presented on Fig. 3b, an absorption peak near 400 nm is seen. It is due to a feature in the bulk interband absorption and is also observed from unstructured surfaces. For short grooves, the plasmonic peaks overlaps with the interband absorption feature and became distinct for $D > 175$ nm. Full 3D Maxwell calculations of the reflectivity spectra obtained on the basis of ellipsometry data strongly corroborate with experimental results.

In another series of experiments, we investigated the optical response and cathodoluminescence (CL) spectra of gratings fabricated on the surface of topological insulator. The periods P of gratings were chosen for their diffraction peaks to be located at different wavelengths from the UV to visible parts of the spectrum. The width of the grating ridge was maintained to be the half the grating period P . 70 nm deep gratings with the periods, P from 200 nm to 1500 nm, were fabricated on the surface of a bulk BSTS crystal as shown in Fig. 2c. The plasmonic response was found in the gratings when they were illuminated with the polarization perpendicular to the grating rulings as shown in Fig. 4a. In contrast to the featureless absorption spectra for the parallel polarization, the formation and evolution of 1st and 2nd-order peaks were clearly seen for the perpendicular polarization in the wavelengths range between 350 nm and 670 nm. Moreover, peaks were also visible for wavelengths longer than 670 nm.

These results should be compared with our cathodoluminescence (CL) data that have also been successfully used in the past to identify plasmonic response⁴⁹. The gratings were excited with electron beam (waist diameter ~ 50 nm; electron energy 40 keV; beam current ~ 10 nA) of a scanning electron microscope. The electron beam was raster scanned on the area of about $10 \mu\text{m} \times 10 \mu\text{m}$ of each grating. Figure 4b shows the normalized CL spectra from each grating where the CL from the unstructured

crystal surface was subtracted. Peaks in the range from 230 nm to 1050 nm can be observed. The emission peaks and their red-shift with increase of the grating period are clearly observed. Importantly, CL peaks' positions accurately match that of the absorption peaks emphasizing their common plasmonic nature of the responses (Fig. 4c). Here, we argue that the observation of the CL peaks for wavelengths beyond 670 nm, i.e. beyond the range of wavelengths where dielectric permittivity of the bulk is negative, is a clear evidence of plasmonic contribution of the surface topological conductivity state.

In summary, we have demonstrated the plasmonic behavior of a topological insulator, $\text{Bi}_{1.5}\text{Sb}_{0.5}\text{Te}_{1.8}\text{Se}_{1.2}$, at optical frequencies. It resulted from a combination of contributions from the topologically protected surface conducting state and a strong dispersion due to the interband transition. The optical and electron beam excitation of the material demonstrated the existence of the plasmonic response with quality factor of about six that is sufficient for many sensors, light localization and metamaterials applications and that outperforms the noble metals in the UV-blue-green parts of the spectrum. We believe that the importance of our results is in the identification of new class of materials with high-frequency plasmonic response where plasmonic functionality can be directly integrated with electronics thanks to the semiconductor nature of the material.

Acknowledgments

The authors would like to thank Jonathan Maddock for assistance with ellipsometry and Cesare Soci, Nikitas Papisimakis, Kevin MacDonald and Yidong Chong for discussion. This work was supported by the Royal Society (UK), EPSRC (UK) Programme on Nanostructured Photonic Metamaterials and Ministry of Education Singapore, research project (Grant No. MOE2011-T3-1-005)

References

- * Electronic address: js1m10@orc.soton.ac.uk
- 1. I. Freestone, N. Meeks, M. Sax, and C. Higgitt, "The lycurgus cup-a roman nanotechnology," *Gold Bulletin*, vol. 40, no. 4, pp. 270–277, 2007.
- 2. A. Kirilyuk, A. V. Kimel, and T. Rasing, "Ultrafast optical manipulation of magnetic order," *Reviews of Modern Physics*, vol. 82, no. 3, p. 2731, 2010.
- 3. A. Tsiatmas, E. Atmatzakis, N. Papisimakis, V. Fedotov, B. Lukyanchuk, N. I. Zheludev, and F. de Abajo, "Optical generation of intense ultrashort magnetic pulses at the nanoscale," *arXiv preprint arXiv:1303.6072*, 2013.
- 4. H. A. Atwater and A. Polman, "Plasmonics for improved photovoltaic devices," *Nature materials*, vol. 9, no. 3, pp. 205–213, 2010.
- 5. J. Attridge, P. Daniels, J. Deacon, G. Robinson, and G. Davidson, "Sensitivity enhancement of optical im-

- munosensors by the use of a surface plasmon resonance fluoroimmunoassay,” *Biosensors and bioelectronics*, vol. 6, no. 3, pp. 201–214, 1991.
6. E. Ozbay, “Plasmonics: merging photonics and electronics at nanoscale dimensions,” *Science*, vol. 311, no. 5758, pp. 189–193, 2006.
 7. D. K. Gramotnev and S. I. Bozhevolnyi, “Plasmonics beyond the diffraction limit,” *Nature Photonics*, vol. 4, no. 2, pp. 83–91, 2010.
 8. D. Miller, “Device requirements for optical interconnects to silicon chips,” *Proceedings of the IEEE*, vol. 97, no. 7, pp. 1166–1185, 2009.
 9. V. R. Almeida, C. A. Barrios, R. R. Panepucci, and M. Lipson, “All-optical control of light on a silicon chip,” *Nature*, vol. 431, no. 7012, pp. 1081–1084, 2004.
 10. P. R. West, S. Ishii, G. V. Naik, N. K. Emani, V. M. Shalaev, and A. Boltasseva, “Searching for better plasmonic materials,” *Laser & Photonics Reviews*, vol. 4, no. 6, pp. 795–808, 2010.
 11. G. V. Naik, V. M. Shalaev, and A. Boltasseva, “Alternative plasmonic materials: Beyond gold and silver,” *Advanced Materials*, 2013.
 12. A. Grigorenko, M. Polini, and K. Novoselov, “Graphene plasmonics,” *Nature Photonics*, vol. 6, no. 11, pp. 749–758, 2012.
 13. J. B. Pendry, “Negative refraction makes a perfect lens,” *Physical review letters*, vol. 85, no. 18, p. 3966, 2000.
 14. C. M. Soukoulis and M. Wegener, “Past achievements and future challenges in the development of three-dimensional photonic metamaterials,” *Nature Photonics*, vol. 5, no. 9, pp. 523–530, 2011.
 15. M. Wuttig and N. Yamada, “Phase-change materials for rewriteable data storage,” *Nature materials*, vol. 6, no. 11, pp. 824–832, 2007.
 16. T. Arakane, T. Sato, S. Souma, K. Kosaka, K. Nakayama, M. Komatsu, T. Takahashi, Z. Ren, K. Segawa, and Y. Ando, “Tunable dirac cone in the topological insulator $\text{Bi}_{2-x}\text{Sb}_x\text{Te}_{3-y}\text{Se}_y$,” *Nature Communications*, vol. 3, p. 636, 2012.
 17. B. Xia, P. Ren, A. Sulaev, P. Liu, S.-Q. Shen, and L. Wang, “Indications of surface-dominated transport in single crystalline nanoflake devices of topological insulator $\text{Bi}_{1.5}\text{Sb}_{0.5}\text{Te}_{1.8}\text{Se}_{1.2}$,” *Physical Review B*, vol. 87, no. 8, p. 085442, 2013.
 18. S. A. Maier, *Plasmonics: fundamentals and applications*. Springer, 2007.
 19. K. H. Kim, K. C. Park, and D. Y. Ma, “Structural, electrical and optical properties of aluminum doped zinc oxide films prepared by radio frequency magnetron sputtering,” *Journal of Applied Physics*, vol. 81, no. 12, pp. 7764–7772, 1997.
 20. I. Hamberg and C. G. Granqvist, “Evaporated sn-doped In_2O_3 films: Basic optical properties and applications to energy-efficient windows,” *Journal of Applied Physics*, vol. 60, no. 11, pp. R123–R160, 1986.
 21. A. J. Hoffman, L. Alekseyev, S. S. Howard, K. J. Franz, D. Wasserman, V. A. Podolskiy, E. E. Narimanov, D. L. Sivco, and C. Gmachl, “Negative refraction in semiconductor metamaterials,” *Nature materials*, vol. 6, no. 12, pp. 946–950, 2007.
 22. S. Law, D. Adams, A. Taylor, and D. Wasserman, “Mid-infrared designer metals,” *Optics Express*, vol. 20, no. 11, pp. 12 155–12 165, 2012.
 23. A. Frölich and M. Wegener, “Spectroscopic characterization of highly doped zno films grown by atomic-layer deposition for three-dimensional infrared metamaterials[invited],” *Optical Materials Express*, vol. 1, no. 5, pp. 883–889, 2011.
 24. K. Santiago, R. Mundle, C. B. Samantaray, M. Bahoura, and A. Pradhan, “Nanopatterning of atomic layer deposited al: Zno films using electron beam lithography for waveguide applications in the nir region,” *Optical Materials Express*, vol. 2, no. 12, pp. 1743–1750, 2012.
 25. M. Noginov, L. Gu, J. Livenere, G. Zhu, A. Pradhan, R. Mundle, M. Bahoura, Y. A. Barnakov, and V. Podolskiy, “Transparent conductive oxides: Plasmonic materials for telecom wavelengths,” *Applied Physics Letters*, vol. 99, no. 2, pp. 021 101–021 101, 2011.
 26. G. V. Naik, J. Liu, A. V. Kildishev, V. M. Shalaev, and A. Boltasseva, “Demonstration of al: Zno as a plasmonic component for near-infrared metamaterials,” *Proceedings of the National Academy of Sciences*, vol. 109, no. 23, pp. 8834–8838, 2012.
 27. G. V. Naik, J. L. Schroeder, X. Ni, A. V. Kildishev, T. D. Sands, and A. Boltasseva, “Titanium nitride as a plasmonic material for visible and near-infrared wavelengths,” *Optical Materials Express*, vol. 2, no. 4, pp. 478–489, 2012.
 28. G. V. Naik, J. Kim, and A. Boltasseva, “Oxides and nitrides as alternative plasmonic materials in the optical range [invited],” *Optical Materials Express*, vol. 1, no. 6, pp. 1090–1099, 2011.
 29. D. Steinmüller-Nethl, R. Kovacs, E. Gornik, and P. Röthhammer, “Excitation of surface plasmons on titanium nitride films: determination of the dielectric function,” *Thin solid films*, vol. 237, no. 1, pp. 277–281, 1994.
 30. A. P. Hibbins, J. R. Sambles, and C. R. Lawrence, “Surface plasmon-polariton study of the optical dielectric function of titanium nitride,” *journal of modern optics*, vol. 45, no. 10, pp. 2051–2062, 1998.
 31. M. Cortie, J. Giddings, and A. Dowd, “Optical properties and plasmon resonances of titanium nitride nanostructures,” *Nanotechnology*, vol. 21, no. 11, p. 115201, 2010.
 32. T. N. Theis, “Plasmons in inversion layers,” *Surface Science*, vol. 98, no. 1, pp. 515–532, 1980.
 33. B. Van Wees, H. Van Houten, C. Beenakker, J. G. Williamson, L. Kouwenhoven, D. Van der Marel, and C. Foxon, “Quantized conductance of point contacts in a two-dimensional electron gas,” *Physical Review Letters*, vol. 60, no. 9, p. 848, 1988.
 34. O. Ambacher, J. Smart, J. Shealy, N. Weimann, K. Chu, M. Murphy, W. Schaff, L. Eastman, R. Dimitrov, L. Wittmer *et al.*, “Two-dimensional electron gases induced by spontaneous and piezoelectric polarization charges in n-and ga-face algan/gan heterostructures,” *Journal of Applied Physics*, vol. 85, no. 6, pp. 3222–3233, 1999.
 35. J. Chen, M. Badioli, P. Alonso-González, S. Thongrattanasiri, F. Huth, J. Osmond, M. Spasenović, A. Centeno, A. Pesquera, P. Godignon *et al.*, “Optical nano-imaging of gate-tunable graphene plasmons,” *Nature*, 2012.
 36. H. Yan, T. Low, W. Zhu, Y. Wu, M. Freitag, X. Li, F. Guinea, P. Avouris, and F. Xia, “Damping pathways of mid-infrared plasmons in graphene nanostructures,” *Nature Photonics*, vol. 7, no. 5, pp. 394–399, 2013.
 37. F. H. Koppens, D. E. Chang, and F. J. Garcia de Abajo, “Graphene plasmonics: a platform for strong

- light-matter interactions,” *Nano letters*, vol. 11, no. 8, pp. 3370–3377, 2011.
38. S. D. Sarma and E. Hwang, “Collective modes of the massless dirac plasma,” *Physical review letters*, vol. 102, no. 20, p. 206412, 2009.
 39. P. Di Pietro, M. Ortolani, O. Limaj, A. Di Gaspare, V. Giliberti, F. Giorgianni, M. Brahlek, N. Bansal, N. Koirala, S. Oh *et al.*, “Observation of dirac plasmons in a topological insulator,” *Nature nanotechnology*, vol. 8, no. 8, pp. 556–560, 2013.
 40. G. Jellison and F. Modine, “Parameterization of the optical functions of amorphous materials in the interband region,” *Applied Physics Letters*, vol. 69, no. 3, pp. 371–373, 1996.
 41. A. Akrap, M. Tran, A. Ubaldini, J. Teyssier, E. Giannini, D. Van Der Marel, P. Lerch, and C. C. Homes, “Optical properties of $\text{Bi}_2\text{Te}_2\text{Se}$ at ambient and high pressures,” *Physical Review B*, vol. 86, no. 23, p. 235207, 2012.
 42. P. Drude, “Zur elektronentheorie der metalle,” *Annalen der Physik*, vol. 306, no. 3, pp. 566–613, 1900.
 43. Y. Sharma and P. Srivastava, “First-principles study of electronic and optical properties of bise in its trigonal and orthorhombic phases,” in *AIP Conference Proceedings*, vol. 1249, 2010, p. 183.
 44. Y. Sharma, P. Srivastava, A. Dashora, L. Vadkhiya, M. Bhayani, R. Jain, A. Jani, and B. Ahuja, “Electronic structure, optical properties and compton profiles of Bi_2S_3 and Bi_2Se_3 ,” *Solid State Sciences*, vol. 14, no. 2, pp. 241–249, 2012.
 45. W. Spitzer, D. Kleinman, and D. Walsh, “Infrared properties of hexagonal silicon carbide,” *Physical Review*, vol. 113, no. 1, p. 127, 1959.
 46. E. Loh, “Optical phonons in beo crystals,” *Physical review*, vol. 166, no. 3, p. 673, 1968.
 47. P. B. Johnson and R.-W. Christy, “Optical constants of the noble metals,” *Physical Review B*, vol. 6, no. 12, p. 4370, 1972.
 48. E. D. Palik, *Handbook of Optical Constants of Solids: Index*. Access Online via Elsevier, 1998, vol. 3.
 49. M. Bashevoy, F. Jonsson, A. Krasavin, N. Zheludev, Y. Chen, and M. Stockman, “Generation of traveling surface plasmon waves by free-electron impact,” *Nano letters*, vol. 6, no. 6, pp. 1113–1115, 2006.

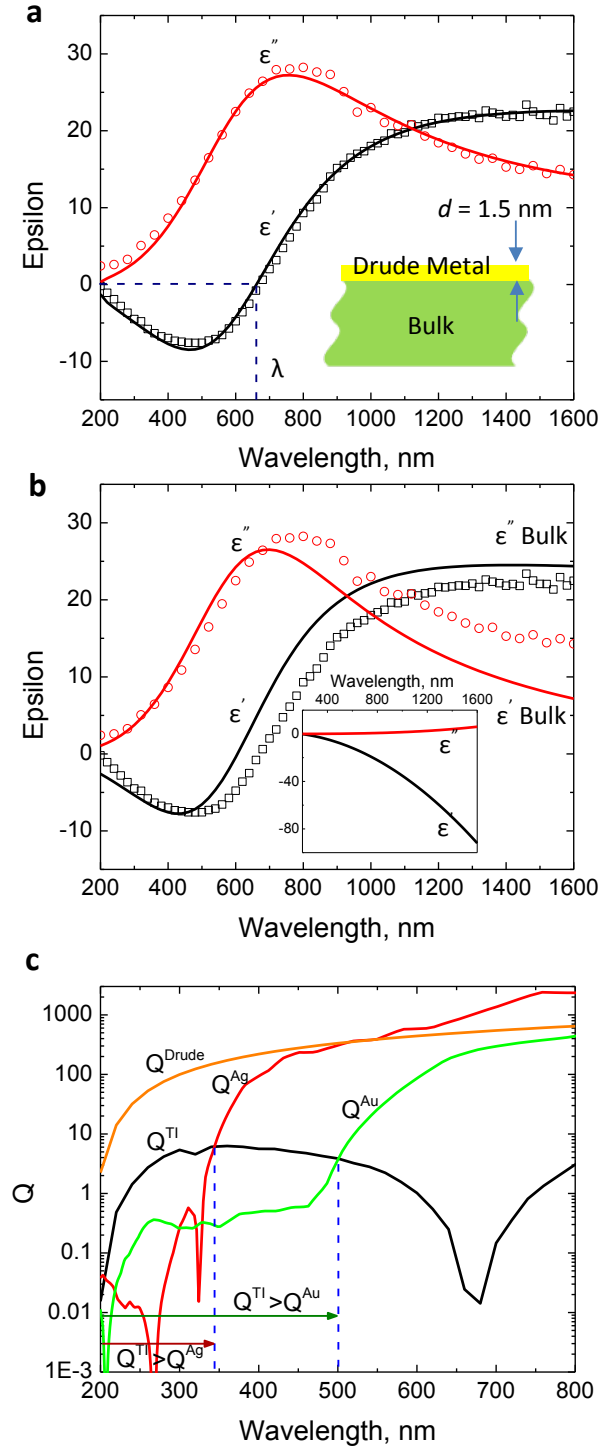


Figure 1: **Plasmonic properties of the $\text{Bi}_{1.5}\text{Sb}_{0.5}\text{Te}_{1.8}\text{Se}_{1.2}$ topological insulator semiconductor in the visible and UV.** (a) Dielectric function of the crystal retrieved from spectroscopic ellipsometry. The inset shows a sketch of the layer-on-bulk model of the crystal with a layer of topological phase of thickness $d = 1.5$ nm. Experimental points are presented together with the modeling data (solid lines); (b) An attempt to fit experimental data by the bulk contribution only (Tauc-Lorentz dispersion formula) show the discrepancy that is attributed to the presence of surface conductivity of topological surface state with a Drude-like dispersion (inset). (c) Figures of merit for surface plasmon polaritons, Q , for the $\text{Bi}_{1.5}\text{Sb}_{0.5}\text{Te}_{1.8}\text{Se}_{1.2}$ crystal, hypothetical Drude metal with properties of the conductive layer on the surface of topological insulator, silver and gold.

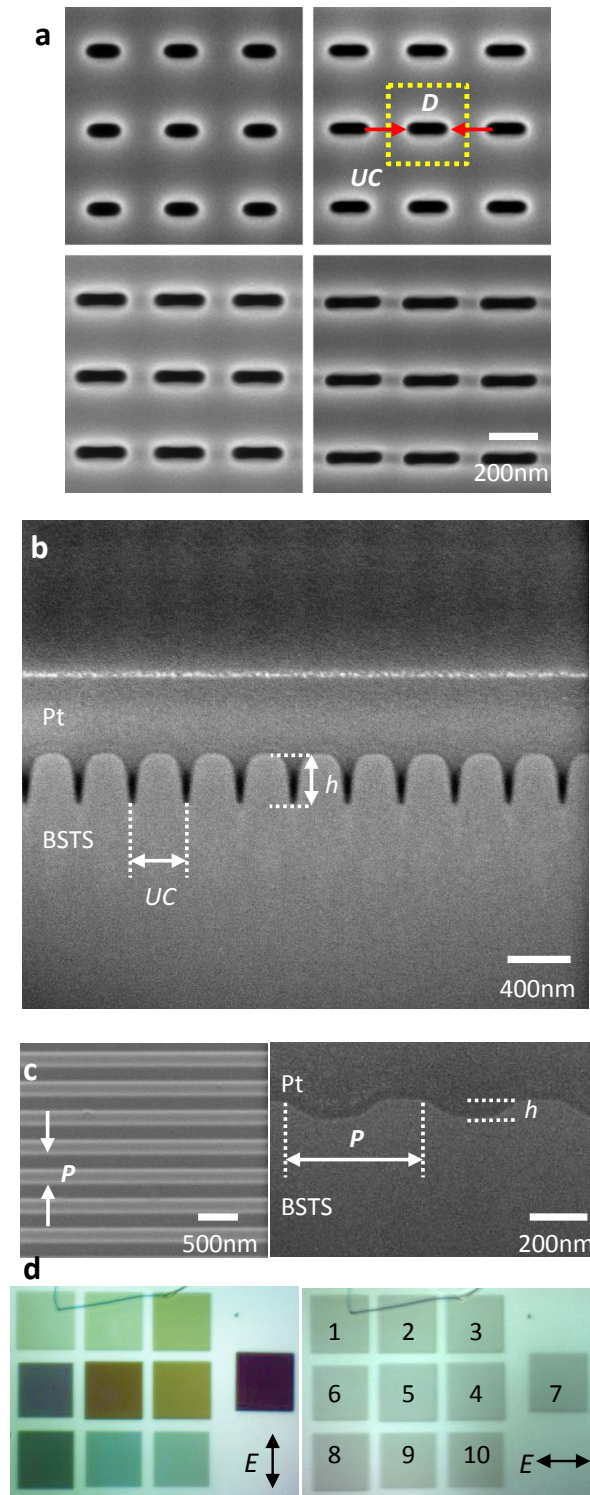


Figure 2: **Nanostructured topological insulator: metamaterial and grating.** (a) SEM images of the nano-slit array metamaterials with nominal lengths of the slits of $D = 125$ nm, 150 nm, 200 nm, and 225 nm. The unit cell (UC) size is 300 nm \times 300 nm; (b) Cross-section of the array perpendicular to the nanoslit shows the slit profile with depth of $h = 300$ nm. Platinum layer was deposited for protection during sectioning; (c) SEM image top view (left) and cross section view (right) of a grating with period $P = 500$ nm and depth $h = 70$ nm; (d) Plasmonic colors can be seen in optical images of nanoslits array with polarized light illumination perpendicular to the slits and are not seen for parallel polarization. Light's polarization is indicated by arrow. Individual sample have sizes of $40 \mu\text{m} \times 40 \mu\text{m}$. The number 1 to 10 on right figure annotate lengths of the nanoslits in the arrays: 1 \leftrightarrow 100 nm, 2 \leftrightarrow 125 nm, 3 \leftrightarrow 150 nm, 4 \leftrightarrow 175 nm, 5 \leftrightarrow 200 nm, 6 \leftrightarrow 225 nm, 7 \leftrightarrow 250 nm, 8 \leftrightarrow 300 nm, 9 \leftrightarrow 350 nm, and 10 \leftrightarrow 400 nm, respectively.

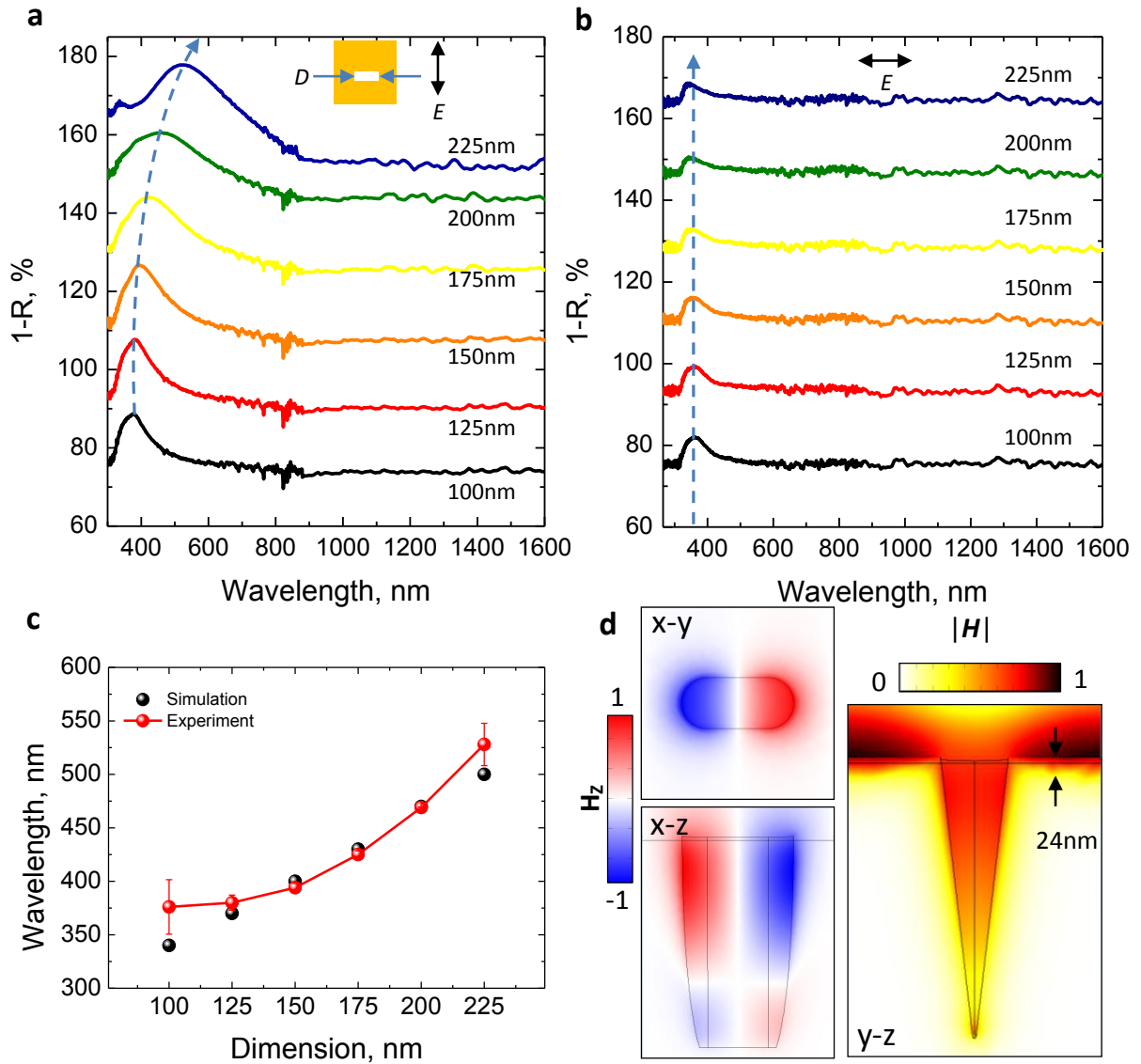


Figure 3: **Plasmonic properties of nano-slit array metamaterials fabricated on topological insulator semiconductor.** (a) Absorption spectra, $1-R$, of various nano-slit arrays with lengths D from 100 nm to 225 nm for light polarized perpendicular to the slits nano-slits and (b) parallel to nano-slits; (c) Peak wavelength of the absorption resonance for various slit lengths increases with the slit length D ; (d) Maxwell modeling of the H_z - and $|H|$ - field distribution in the slit length of 175nm at the resonance wavelength of 430 nm indicates that light is localized in the surface layer of thickness $x \sim 24$ nm (incident light polarization is perpendicular to the nano-slit). Different cross-sections of the slit are shown.

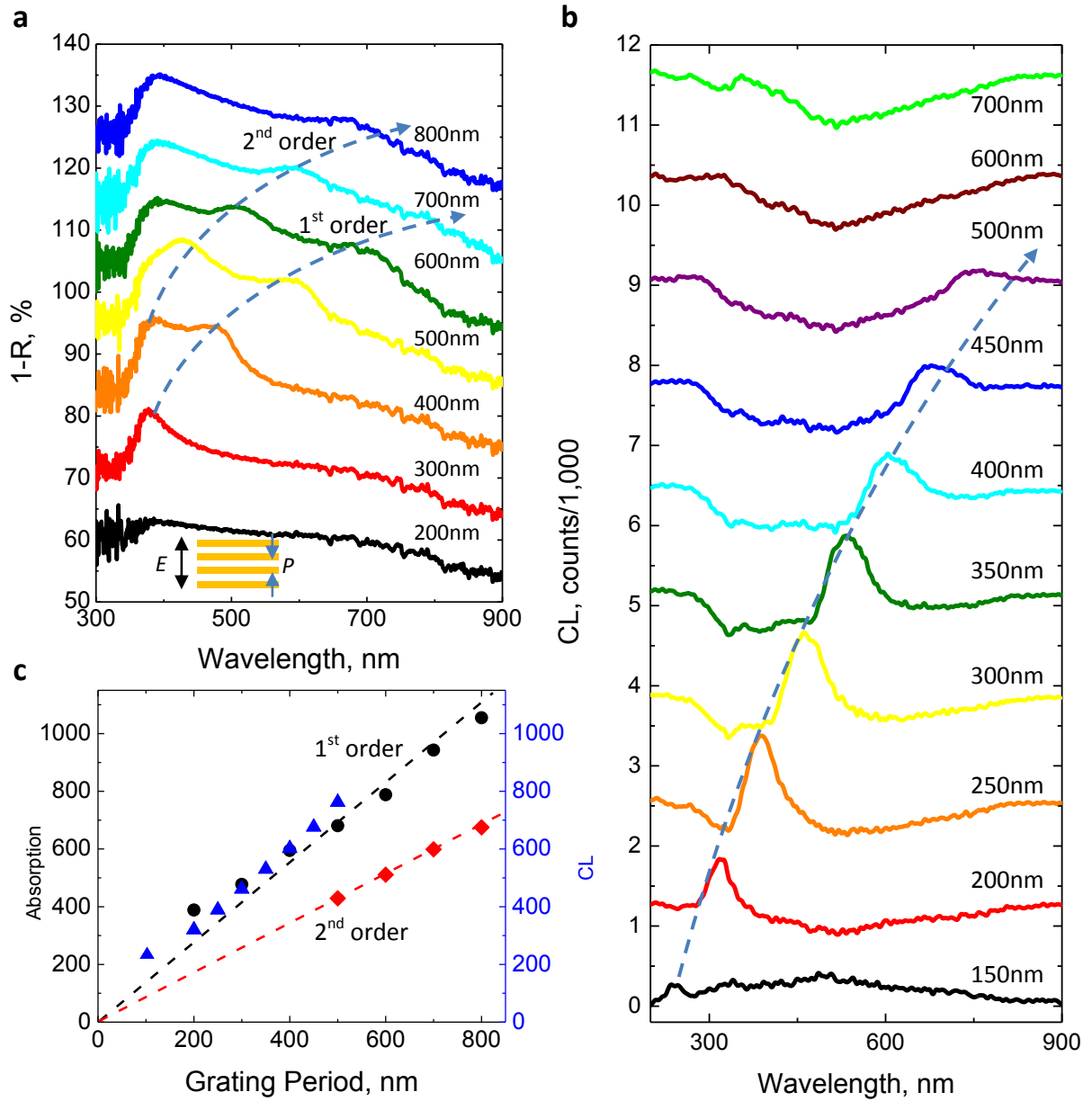


Figure 4: **Plasmonic properties of gratings fabricated on topological insulator semiconductor.** (a) Absorption spectra of one-dimensional gratings with pitch P from 200 to 800 nm, in 100 nm steps for the incident polarizations perpendicular to the grating; (b) Cathodoluminescence spectra of the gratings with period from 150 nm to 700 nm; (c) Peak wavelength of the absorption and CL resonances for various periods of the grating (triangles- CL data; circles and rombs – absorption data).